

Pollution source identification in heterogeneous porous media

Juliana Atmadja

Department of Civil Engineering, Columbia University, New York

Amvrossios C. Bagtzoglou

Departments of Civil Engineering, and Earth and Environmental Engineering, Columbia University, New York

Abstract. The reliable assessment of hazards or risks arising from water contamination problems and the design of efficient and effective techniques to mitigate these problems require the capability to predict the behavior of chemical contaminants in flowing water. Most attempts at quantifying contaminant transport have relied on a solution of some form of the advection-dispersion-reaction equation. In this paper, the Backward Beam Equation (BBE) method is studied and enhanced to solve the Advection-Dispersion Equation (ADE) within a contaminant source identification context. Even though the BBE has been applied successfully to parabolic problems before, it has never been applied to solving the ADE with heterogeneous parameters. The BBE employed in this work is capable of recovering the time history and spatial distribution of a groundwater contaminant plume from measurements of its current position. Using examples involving deterministic heterogeneous dispersion coefficients, we show that the method is robust enough to handle heterogeneous parameters. By altering the method, to produce a hybrid between a marching and a jury method called the Marching-Jury Backward Beam Equation (MJBBE), we were also able to make the problem practical to solve.

1. Introduction

Groundwater amounts to about half of the U.S. population's source of drinking water. Unfortunately, this vital resource is vulnerable to contamination. In the *U.S. Environmental Protection Agency (EPA) 305(b) report [U.S. EPA, 1998a]*, 37 states reported that they found potential sources of groundwater contamination. Major sources of pollution are Underground Storage Tanks (USTs), landfills, septic systems, and hazardous waste sites. Other sources include pesticides, leaks or spills of industrial chemicals at manufacturing facilities, runoff of salt and other chemicals from roads and highways, and fertilizer on agricultural land. Most of water contamination cases occur in highly developed areas, agricultural areas, and industrial zones. As of March 1996, more than 300,000 releases from USTs had been confirmed [*U.S. EPA, 1998b*].

In 1994 the National Academy of Sciences estimated that over a trillion dollars, or approximately \$4000 per person in the United States, will be spent during the next 30 years for cleanup efforts of contaminated soil and groundwater [*U.S. EPA, 1999*]. The cost of cleanup is staggering, and in many cases it is hard to identify which companies or parties are responsible for the contamination due to lack of tools to discover the pollution source. The reliable assessment of contamination problems and the design of efficient and effective techniques to mitigate these problems require the capability to predict the behavior of chemical contaminants in groundwater. Reliable and quantitative predictions of contaminant movements can be made only if we understand the processes controlling transport, advection, hydrodynamic dispersion, and chemical, physical, and biological reactions that affect solute

concentrations in the water. To predict the behavior of contaminants, the effects of each of these influences must be adequately represented in a model or group of models. One area of contaminant behavior that has been researched for quite some time is the chemical behavior aspect. Chemical fingerprinting has been a major element in environmental investigations used to identify the contaminants found in groundwater. However, fingerprinting alone is not always sufficient to provide answers to questions of source and responsibility [*Stout et al., 1998*]. In most cases, additional information such as the release and spill history of the contaminant is needed. Furthermore, by accurately identifying pollution sources, the time and cost requirements associated with the complex and lengthy process of remediation can be dramatically reduced.

Most attempts at quantifying contaminant transport have relied on solving some form of a well-known governing equation referred to as advection-dispersion-reaction equation. In identifying the source of pollution we have to solve the governing equations backward in time. Modeling contaminant transport using reverse time is an ill-posed problem since the process, being dispersive, is irreversible. Because of this ill-posedness, the problems have discontinuous dependence on data and are sensitive to the errors in data. A problem is categorized as a well-posed problem if (1) the solution exists, (2) the solution is unique, and (3) the problem is stable [*Tikhonov and Arsenin, 1977*]. Problems that do not satisfy these criteria are called ill-posed. For the groundwater contamination problem the plume has to have originated from someplace, therefore, physically, the plume exists. However, in mathematically rigorous terms, the fact that we have a present-day plume concentration does not necessarily mean that we satisfy the existence criterion. The solution exists only when we have perfect and consistent model and data that satisfy extremely restrictive conditions. Meeting the stability criterion is a difficult task to accomplish since numerical schemes that are

Copyright 2001 by the American Geophysical Union.

Paper number 2001WR000223.
0043-1397/01/2001WR000223\$09.00

usually implemented as a marching procedure are unstable for a negative time step, and make it impossible to run contaminant transport problems backward in time. As for the non-uniqueness of the solution, there is no method that can bypass this inherent problem. In inverse problems one of the common practices to overcome the stability and nonuniqueness problems is to make assumptions about the nature of the unknown function so that the finite amount of data in observations is sufficient to determine that function. This can be achieved by converting the ill-posed problem to a properly posed one by stabilization or regularization methods. In the case of groundwater pollution source identification, most of the time we have additional information available such as the location of potential release sites and chemical fingerprints of the plume. In this paper, the Backward Beam Equation (BBE) method, originally proposed by *Carasso* [1972] and *Buzbee and Carasso* [1973], was studied and enhanced to reconstruct the release history and the spatial distributions of contaminant plumes.

2. Literature Review on Methods Used for Groundwater Pollution Source Identification

For the past 15 years several attempts have been made to solve the Advection-Dispersion Equation (ADE) backward in time in order to identify pollution sources. One of the early methods used to backtrack the pollution source location is to run forward simulations and check the solutions with the measured/current spatial data observed. Owing to the nonuniqueness of the solution and the infinite number of plausible combinations, one needs to follow an optimization method to obtain the best fitted solution. Among the first people to tackle pollution source identification problems using optimization approaches are *Gorelick et al.* [1983]. They formulated the groundwater pollution source identification as forward-time simulations in conjunction with an optimization model using linear programming and multiple regressions. In their work, *Gorelick et al.* assumed no uncertainty in the physical parameters of the aquifer. The method used was also restricted to cases where data are available in the form of breakthrough curves.

Another optimization approach was followed by *Wagner* [1992]. *Wagner* developed a methodology for performing simultaneous model parameter estimation and source characterization, in which he used an inverse model as a nonlinear maximum likelihood estimation problem. Along the same line of work, *Mahar and Datta* [1997, 2001] developed a methodology that combines the concepts of optimal identification of pollutant sources with the optimal design of groundwater quality monitoring networks for an efficient identification process. They applied their method to a hypothetical two-dimensional (2-D) homogeneous, isotropic, and saturated aquifer with a conservative pollutant plume. *Mahar and Datta* [2000] also used a nonlinear optimization to estimate the magnitude, location, and duration of groundwater pollution sources under transient conditions.

Bagtzoglou [1990] and *Bagtzoglou et al.* [1991, 1992] are among the first to attempt solving the ADE backward in time without relying on optimization approaches. In their work, they modeled the reversed time transport equation using random walk particle methods, for which the advective part of the transport model is reversed while the dispersive part is left unchanged. They presented a probabilistic framework to iden-

tify solute sources in heterogeneous media. Repeated reversed time solute transport simulations with evaluation of the first two moments of the concentration probability density function (pdf) were conducted. Using geostatistical techniques, they successfully assessed the relative importance of each potential source.

In the line of probabilistic approaches, *Wilson and Liu* [1994] solved the transport using stochastic differential equations backward in time. As in the method of *Bagtzoglou et al.*, *Wilson and Liu* also kept the dispersion part positive and reversed the advection part. They provided two types of maps, namely, travel time probability and location probability maps. *Wilson and Liu* showed that both location and travel time probabilities could be calculated directly, using a backward-in-time version of traditional continuum advection-dispersion modeling. An extension of their study for a 2-D heterogeneous aquifer was reported by *Liu and Wilson* [1995]. The results for travel time probability are in very close agreement with the simulation results from traditional forward-in-time methods. Results from this model were verified by *Neupauer and Wilson* [1999] using the adjoint method. In this method the forward governing equation, with concentration as the dependent variable, is replaced by the adjoint equation, with the adjoint state as the dependent variable. These researchers showed that backward-in-time location and travel time probabilities are adjoint states of the forward-in-time resident concentration.

Snodgrass and Kitanidis [1997] also used a probabilistic approach combining Bayesian theory and geostatistical techniques. In their approach the source function to be estimated is discretized into components that are assigned a known stochastic structure with unknown stochastic parameters. The method incorporates uncertainty in contaminant concentration. *Snodgrass and Kitanidis'* method is an improvement to some other methods in that the solutions are more general and make no blind assumptions about the nature and structure of the unknown source function. This approach was used for cases for which the location of the potential source was known a priori.

A different approach was proposed by *Skaggs and Kabala* [1994]. They attempted to reconstruct the history of the plume using Tikhonov Regularization (TR). *Skaggs and Kabala* studied a one-dimensional (1-D) solute transport problem through a saturated homogeneous medium with a complex contaminant release history and assumed no prior knowledge of the release function. This method was very effective when there existed adequate data. Later, *Liu and Ball* [1999] used *Skaggs and Kabala's* modified TR technique to study a contaminant release at Dover Air Force Base (AFB), Delaware. They used field measured concentration profiles in low-permeability porous media that underlie a contaminated aquifer at Dover AFB. For the two principal chemical contaminants, PCE and TCE, the Tikhonov method gave similar results as the measured data for PCE.

Skaggs and Kabala [1995] employed the Quasi-Reversibility (QR) method for the same problem solved using their TR method. In the QR method, *Skaggs and Kabala* solved an equation that is close to the original governing equation and which is stable with a negative time step. The diffusion operator $\partial/\partial t - \Delta$ was replaced by $\partial/\partial t - \Delta - \varepsilon\Delta^2$. A moving coordinate system was used to account for the velocity term of the ADE. The results are less accurate than that of the TR approach, but it is computationally less expensive. The authors claimed that it is much easier to incorporate heterogeneous

parameters in the QR method. However, up to today, heterogeneous parameters have not been incorporated either in the QR method or in the Tikhonov method.

Another approach, namely, a Minimum Relative Entropy (MRE) inversion was used by *Woodbury and Ulych* [1996]. The MRE inversion is a method of statistical inference. Given prior information in terms of a lower and upper bound, a prior bias, and constraints in terms of measured data, the MRE provides exact expressions for the posterior pdf and expected value of the inverse problem. The plume source is also characterized by a pdf. The problem solved in their study is the same as Skaggs and Kabala's problem. For the noise-free data the MRE was able to reconstruct the plume evolution history indistinguishable from the true history. As for data with noise, the MRE managed to recover the salient features of the source history. *Woodbury et al.* [1998] extended the MRE approach to reconstruct a three-dimensional (3-D) plume source within a 1-D constant velocity field and constant dispersivity system.

Recently, *Neupauer et al.* [2000] performed a study to compare the TR and the MRE methods. They found that both methods perform well in reconstructing a smooth source function. For an error free step function source history the MRE performs better than the TR. On the other hand, the TR method is more robust in handling data that contain measurement errors.

Recently, *Skaggs and Kabala* [1998] extended their study of TR using Monte Carlo simulation to answer the question of how far back one can use the TR procedure in recovering the release history of the plume, since the procedure always produces a recovered release curve that accurately reproduces the data.

Another recent study was conducted by *Birchwood* [1999], in which he used a Fourier-based inverse technique to recover the source location and release history of the groundwater contaminant plume from breakthrough curve data obtained at a single monitoring well. The Birchwood model is capable of finding the potential release sites by imposing a causality requirement upon the release history and carefully interpreting the multiple solutions that arise thereafter. In this method the breakthrough curve is represented as a Fourier series whose coefficients are expressed as functions of the release location and the Fourier coefficients of the release history. The release location is determined by imposing a condition of causality upon the release history. Recovery of the source location and profile of the unit pulse release history with homogeneous parameters was used to demonstrate the method. Birchwood concluded that preliminary results suggest that the method is capable of quantifying the location coordinate of a pollution source to a reasonable degree of accuracy, but the results are highly sensitive to the accuracy of the inferred source location.

The latest approach in recovering the release history was proposed by *Alapati and Kabala* [2000]. They used the Nonlinear Least Squares (NLS) method after a successful task performed by *MacDonald* [1995], who applied the method to invert a 1-D pure diffusion problem. MacDonald applied the method to recover a number of Dirac-delta sources with large measurement errors in the data. *Alapati and Kabala* [2000] solved a problem similar to the *Skaggs and Kabala* [1994] test case using the NLS method without regularization. They found that the solution was very sensitive to noise and to the extent to which the plume has been dissipated. Another recent paper by *Morrison* [2000] presented an extensive literature review of

commonly used environmental forensic methods for age dating and source identification.

In summary, in all previous studies there exist two broad classes of approaches used in identifying groundwater pollution sources. One class is employing probabilistic techniques such as geostatistics to deduce the probability of the location of the sources. The other class is using deterministic direct methods to solve the governing equations backward in time in order to reconstruct the release history of the contaminant plume. However, in the class of direct method approaches, only problems with constant parameters are solved. In addition to hydrogeologists, mathematicians have been attracted to solve ill-posed problems for partial differential equations for some time. Among the methods developed for solving such ill-posed problems is the Backward Beam Equation (BBE) method, first developed by *Carasso* [1972]. The BBE method implementation for heat equation problems was originally proposed by *Buzbee and Carasso* [1973]. The method is applicable to mixed problems with variable coefficients that may also depend on time. However, the BBE has never been demonstrated to work in such cases. The physical and mathematical models of heat and mass transfer are similar. Therefore, in the work presented herein, this method is studied and enhanced to solve the ADE with heterogeneous parameters and within a contaminant source identification context and with computational efficiency in mind.

3. Development of the Marching-Jury Backward Beam Equation Method

The BBE was first developed by *Carasso* [1972] to solve mixed parabolic initial boundary problems over long time intervals. The method has been used in the past by *Buzbee and Carasso* [1973] to solve linear self-adjoint parabolic problems backward in time. In addition, the BBE method was also used by *Carasso* [1975] in obtaining the solutions to the final value problem of Burger's equation. In a forward in time problem, for large time intervals, that is $t \rightarrow \infty$, one can assume that the solution reaches a known steady state value, and one might have an approximate value of the forward solution at $t = T_{ft}$. Unfortunately, for this type of problem, not all numerical schemes which are unconditionally stable for the direct problem (such as the implicit and Crank-Nicolson schemes) give correct solutions. Carasso suggested that with an extra data point, from having values at $t = T_{ft}$, it is feasible to consider the use of elliptic boundary value techniques as a solution. His interest in the BBE method stemmed from the fact that a solution of the heat equation $f_t = f_{xx}$ also satisfies $f_{tt} = f_{xxxx}$.

The 1-D problem can be described as follows:

$$\partial f / \partial t = -\mathcal{L}_o f, \quad 0 < x < L, \quad t > 0 \quad (1)$$

subject to

$$f(x, 0) = f_1(x), \quad f(x, T_{ft}) = f_2(x), \quad 0 \leq x \leq L \quad (2)$$

$$f(0, t) = 0, \quad f(L, t) = 0, \quad t \geq 0, \quad (3)$$

where \mathcal{L}_o is a differential operator in space. In the case of a mixed parabolic problem the space differential operator is

$$\mathcal{L}_o f \equiv -[a(x)f_x]_x + c(x)f. \quad (4)$$

In general, we will be given values of $f_1(x)$ for initial value problems or $f_2(x)$ for final value problems, but not both $f_1(x)$

and $f_2(x)$. The most common numerical method for solving initial value problems is to use a marching procedure, during the implementation of which we approximate the solution of a problem at time $t = (n + 1)\Delta t$ from a corresponding previous approximation at $t = n\Delta t$, where n is the time discretization. However, there is a restriction on the value of Δt for the method to be stable; that is, the value cannot be negative. Unfortunately, in solving a final value problem we need to march the solution backward, which implies using a negative Δt . Carasso developed a stable algorithm for the backward problem, which is not a marching procedure, but a “jury” or “boundary value” scheme. The jury procedure is employed by transforming the governing equation to a backward beam equation. We will call the original BBE method as Jury BBE (JBBE). In using this procedure we need to supply the initial, $f_1(x)$, and terminal data, $f_2(x)$. Using the JBBE method means that we are calculating the solution of the problem simultaneously in space and time ($\Omega \times [0, T_{fi}]$) where $\Omega = [0, L]$. Because of this requirement, solving a 1-D problem is the same as solving a 2-D problem. The JBBE method is a two-point boundary value problem, and it therefore requires massive computational effort to solve, especially for 2-D and 3-D domains. The computational effort for the jury method is proportional to $O(N_g^2 \times N_t^2)$, where N_g and N_t are the number of space and time discrete points, respectively. Even though the computational effort requirement seems to be massive, this method was considered for groundwater pollution source identification primarily because the behavior of the solution to the BBE is insensitive to the direction of time.

The JBBE can be obtained by differentiating (1) and the corresponding boundary conditions with respect to t . Assuming a homogeneous diffusion case, that is, $\alpha(x) = 1$ and $c(x) = 0$ in (4), our governing equation becomes

$$\partial f / \partial t = -\mathcal{L}_d f = f_{xx}. \tag{5}$$

The auxiliary equation is obtained by taking the derivative of (5) with respect to time:

$$f_{tt} = -\mathcal{L}_d f_t = \mathcal{L}_d^2 f = f_{xxxx} \tag{6}$$

and the corresponding initial and terminal and boundary conditions become

$$f(0, t) = f_{xx}(0, t) = f(L, t) = f_{xx}(L, t) = 0, \quad t \geq 0 \tag{7}$$

$$f(x, 0) = f_1, \quad f(x, T_{fi}) = f_2. \tag{8}$$

The auxiliary problem is called the backward beam equation due to its similarity with the equation of a vibrating beam, $v_{tt} + v_{xxxx} = 0$, with the sign reversed. When one deals with 2-D parabolic problems, the differential operator in space is

$$\mathcal{L}_o \equiv -([a(x, y) f_x]_x + [b(x, y) f_y]_y). \tag{9}$$

Again, for homogeneous parameters one can assume $\alpha(x, y) = b(x, y) = 1$ and by differentiating (1) with respect to t , the following auxiliary problem is obtained:

$$f_{tt} = f_{xxxx} + 2f_{xyy} + f_{yyy}. \tag{10}$$

Equation (10) is similar to the plate equation of motion, $v_{tt} = -[v_{xxxx} + 2v_{xyy} + v_{yyy}]$. Owing to its apparent similarity with the plate equation of motion, we call (10) the Backward Plate Equation (BPE), and it will be the subject of a forthcoming

paper. In the present paper, however, we will concentrate on 1-D cases only.

The backward problem associated with (5) is as follows: given known function $f_2(x)$ and assuming $f_1(x)$ to be unknown, find a solution of (5) at different times. For a backward problem we set $t = T_{fi} \equiv T_{bi}$ as our present-day or initial time and $t = 0 = T_{ft} \equiv T_{bt}$ as our terminal time (i.e., the terminal condition of a forward solution will be equal to the initial condition of a backward solution and vice versa). In general, the solution of the problem at $t = T_{fi}$ is not known perfectly. In real problems one can measure the present-day distribution of the temperature, concentration, or any other scalar represented by f . From these measurements one can then fit an equation to the distribution. It is generally possible to calculate a bound on the errors generated by this procedure. Let such a bound be

$$\|f(T_{bi}) - f_2\|_2 \leq \delta \tag{11}$$

for the initial data, where δ can be chosen to be the error between the measured and the exact values. Let the bound in the resulting errors in the terminal data be

$$\|f(T_{bt}) - f_1\|_2 \leq M, \tag{12}$$

where M is the acceptance level for the errors in the predicted terminal values.

Since $f_1(x)$ is unknown, we will assume $f_1 = 0$, that is, assuming the wrong terminal data. To reduce errors in the reverse time solution caused by assuming $f_1 = 0$, we first examine how these errors are likely to grow by considering the direct problem in which solutions of (5) are obtained by marching from the initial condition $f_1(x) = \tilde{f}_1(x)$. If $\tilde{f}_1(x)$ contained errors, these could potentially decay more slowly with time than the solutions of (5) that decay exponentially with time. Thus, eventually, a time would be reached where the error would be greater than the solution itself. If the solutions of (5) were to grow exponentially sufficiently fast, the error due to the wrong initial data would eventually be imperceptible. Thus, rather than dealing with (5) directly, we can set

$$w = e^{kf}, \quad 0 \leq t \leq T_{bi}, \tag{13}$$

where

$$k = (1/T_{bi}) \ln (M/\delta) \tag{14}$$

as given by *Buzbee and Carasso* [1973], where δ and M are the bounds defined by (11) and (12), respectively.

Taking first the derivative of (13) with respect to time and substituting (1), we obtain

$$\partial w / \partial t = -(\mathcal{L}_o - k)w \tag{15}$$

and taking the derivative of (15) with respect to time once more, we get the auxiliary problem of (5):

$$\partial^2 w / \partial t^2 = (\mathcal{L}_o - k)^2 w. \tag{16}$$

The corresponding initial and terminal conditions are

$$w(x, T_{bi}) = e^{kT_{bi}} f_2, \quad w(x, 0) = 0. \tag{17}$$

3.1. Implementation of the JBBE for the ADE

Now, for a 1-D heterogeneous ADE, the governing equation is

$$\frac{\partial C}{\partial t} = \frac{\partial}{\partial x} \left[D(x) \frac{\partial C}{\partial x} \right] - \frac{\partial}{\partial x} [u(x)C]. \quad (18)$$

In the case of 1-D heterogeneous contaminant transport, C is the solute concentration, $D(x)$ is the dispersion coefficient, and $u(x)$ is the transport velocity in the x direction. A contaminant plume history would be found by solving (18) subject to

$$C(x_1, t) = C_{in}(t) \quad 0 \leq t \leq T_{bi} \quad (19)$$

$$C(0, t) = C(L, t) = 0 \quad 0 \leq t \leq T_{bi} \quad (20)$$

$$C(x, T_{bi}) = C_T(x) \quad 0 \leq x \leq L, \quad (21)$$

where $C_{in}(t)$ is the unknown contaminant source function at the inlet x_1 and $C_T(x)$ is the observed plume's spatial distribution at time T_{bi} .

Substituting $w = e^{kt}C$, the auxiliary problem corresponding to (18) is

$$\frac{\partial^2 w}{\partial t^2} = \left(\frac{\partial}{\partial x} \left[D(x) \frac{\partial}{\partial x} \right] - \frac{\partial}{\partial x} [u(x)] - k \right)^2 w, \quad (22)$$

$$0 \leq x \leq L, \quad 0 < t < T_{bi}$$

subject to

$$w(0, t) = w(L, t) = 0, \quad t \geq 0 \quad (23)$$

$$w_t(0, t) = w_t(L, t)$$

$$= \left[\frac{\partial}{\partial x} \left[D(x) \frac{\partial}{\partial x} \right] - \frac{\partial}{\partial x} [u(x)] - k \right] w = 0 \quad (24)$$

$$w(x, T_{bi}) = e^{kT_{bi}} f_2(x), \quad w(x, 0) = 0. \quad (25)$$

Let $\mathcal{P} = (\partial/\partial x [D(x) \partial/\partial x] - \partial/\partial x [u(x)] - k)$ and $A = \mathcal{P}^2$. We used a central difference approximation for the $\partial^2/\partial x^2$ and $\partial^2/\partial t^2$ terms and experimented with different approximations for the $\partial/\partial x$ term, using the Central Finite Difference (CFD), first-order Upwind Finite Difference (UFD), and third-order Upwind Finite Difference (3UFD) schemes. Using the central difference approximation for all terms, (22) becomes:

$$\frac{(w^{n+1} - 2w^n + w^{n-1}))}{\Delta t^2} - Aw^n = 0, \quad n = 1, 2, \dots, N_t \quad (26)$$

$$w^{N_t} = e^{kT_{bi}} f_2, \quad w^0 = 0, \quad (27)$$

where the approximation for \mathcal{P} is

$$\mathcal{P} = \frac{1}{\Delta x^2}$$

$$\begin{bmatrix} D_{i+\frac{1}{2}} + D_{i-\frac{1}{2}} & -D_{i+\frac{1}{2}} & & & & & \\ -D_{i-\frac{1}{2}} & D_{i+\frac{1}{2}} + D_{i-\frac{1}{2}} & -D_{i+\frac{1}{2}} & & & & \\ & & \ddots & \ddots & \ddots & & \\ & & & -D_{i-\frac{1}{2}} & D_{i+\frac{1}{2}} + D_{i-\frac{1}{2}} & -D_{i+\frac{1}{2}} & \\ & & & & -D_{i-\frac{1}{2}} & D_{i+\frac{1}{2}} + D_{i-\frac{1}{2}} & \\ & & & & & & \ddots & \ddots & \ddots & & \end{bmatrix} - \frac{1}{2\Delta x} \begin{bmatrix} 0 & -u_{i+1} & & & & & \\ u_{i-1} & 0 & -u_{i+1} & & & & \\ & \ddots & \ddots & \ddots & & & \\ & & u_{i-1} & 0 & -u_{i+1} & & \\ & & & u_{i-1} & 0 & & \end{bmatrix} - k[I] \quad (28)$$

and $D_{i\pm 1/2}$ is the interfacial value of D , obtained by using harmonic averaging:

$$D_{i\pm 1/2} = \frac{2D_i D_{i\pm 1}}{D_i + D_{i\pm 1}}. \quad (29)$$

The boundary conditions (24) are incorporated by adding fictitious points to the left of $x = 0$ and to the right of $x = L$. Once the auxiliary problem is solved for $w(x, t)$, solutions are obtained by applying

$$C(x, t) = e^{-kt} w(x, t). \quad (30)$$

3.2. Implementation of the Marching-Jury Procedure

In order to render the computational problem manageable, we modified the original JBBE method, by marching the method in smaller total time intervals than the JBBE total time requirement. The method is, in essence, a hybrid between a marching and a jury method, hence the name Marching-Jury Backward Beam Equation (MJBBE). The modification of the jury backward beam equation method is as follows.

Instead of using a total time t_{tot} from the initial time T_{bi} to the terminal time T_{bt} ($t_{\text{tot}} = T_{bi} - T_{bt}$), we marched the solution from T_{bi} to an intermediate time t_d , which resulted in a smaller total time ($t_{\text{tot}} = T_{bi} - t_d$) to be solved. For example, if our initial time were $T_{bi} = 2$, and our terminal time were $T_{bt} = 0$, instead of using $t_{\text{tot}} = 2$, we would choose a smaller total time to be solved, for example, $t_{\text{tot}} = 0.5$. In the modified method our initial time $T_{bi} = 2$, and terminal time $T_{bt} = 1.5$. We then choose an interval ΔT for saving our results, for example, $\Delta T = 0.1$. Even though ΔT does not necessarily have to be equal to the time step Δt , we routinely make this assignment for convenience. We will then obtain the solution at $T_{\text{solv}} = T_{bi} - \Delta T$. For our example this means $T_{\text{solv}} = 1.9$. The next step is to use T_{solv} as our initial time T_i and the same t_{tot} and ΔT as chosen before. We will then solve the problem by marching backward in a succession of N_M marching steps, where N_M depends on ΔT . For the above example, to obtain the solution at $T_{\text{target}} = 1.1$ requires $N_M = 9$. By incorporating the marching procedure to the JBBE the computational effort for the method is proportional to $O(N_g^2 \times N_t^2 \times N_M)$. Note that with the implementation of the MJBBE, t_{tot} and therefore the N_t are drastically reduced. The method and the CPU time savings will be presented in greater detail in section 4.

4. Results and Discussion

4.1. MJBBE Results for the Heat Equation

The MJBBE method was tested using a case that has been analyzed previously with the JBBE by a different researcher. The example case is a numerical example of the heat equation presented by Elden [1982], for which the exact solution is known. The direct problem is described as follows:

$$\partial T/\partial t = \partial^2 T/\partial x^2, \quad 0 \leq x \leq \pi, \quad 0 < t < 0.5 \quad (31)$$

$$T(0, t) = T(\pi, t) = 0 \quad (32)$$

$$T(x, 0) = c_1 \sin x + c_3 \sin 3x, \quad 0 \leq x \leq \pi, \quad (33)$$

where

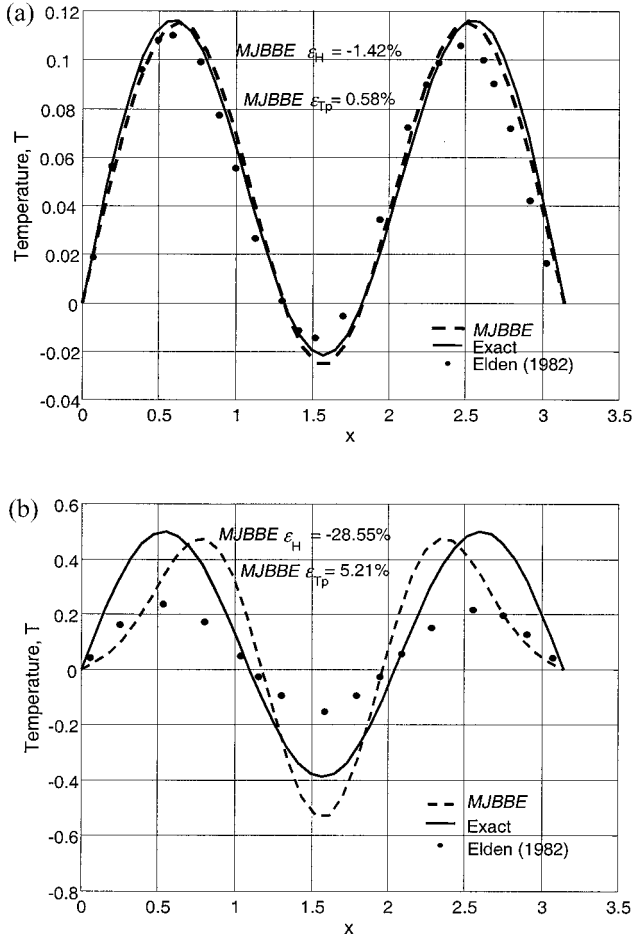


Figure 1. MJBBE method results for Elden's heat equation example at (a) $t_b = 0.5T_{sim}$ and (b) $t_b = 0.88T_{sim}$.

$$c_1 = \sqrt{\frac{2}{\pi}} 0.1 \quad \text{and} \quad c_3 = \sqrt{\frac{2}{\pi}} 0.99. \quad (34)$$

Exact solution for this problem is obtained through separation of variables and is

$$T(x, t) = c_1 e^{-t} \sin x + c_3 e^{-9t} \sin 3x. \quad (35)$$

For each time snapshot, two different error measurements are calculated. They are

(1) heat error, normalized by the exact amount of heat

$$\varepsilon_H = \frac{c\rho \left(\int_x T^a dx - \int_x T^{num} dx \right)}{c\rho \left(\int_x T^a dx \right)} \times 100\% \quad (36)$$

(2) temperature peak error, normalized by the exact peak temperature

$$\varepsilon_{Tp} = \frac{\max(T^a) - \max(T^{num})}{\max(T^a)} \times 100\%, \quad (37)$$

where $\max(\)$ indicates the maximum value of $(\)$ for all grid points in the domain, c is the specific heat, ρ is the density, and

Table 1. Comparison of the Mass and Peak Errors for the Homogeneous ADE Problem Created by JBBE and MJBBE

Time	$\varepsilon_M, \%$		$\varepsilon_P, \%$	
	JBBE	MJBBE	JBBE	MJBBE
$0.2T_{sim}$	-0.33	-0.24	-0.48	-0.19
$0.9T_{sim}$	-1.51	-1.10	-1.74	-0.77

superscripts a and num stand for analytical and numerical values, respectively.

Elden chose $M = \|T(x, 0)\| = 1$ and $\delta = 10^{-6}$ that give an equivalent $k \cong 27.63$ for the MJBBE method. In this study, the problem was run forward from $t = 0$ up to $t = 1$. The result at $t = 1$ was used as the backward initial time $t = T_{bi} = 1$. The total time of simulation (T_{sim}) for this study is $T_{sim} = T_{bi} - T_{bt} = 1 - 0 = 1$. In the analysis we used $\Delta t = 0.005$ and $\Delta x = \pi/40$. Our results differ from that of Elden's because in his study, Elden replaced w_{tt} by a Padé approximation, while we use a central difference approximation. Elden's results at 50% of the total time contained a heat error of about 1.87% and a peak temperature error of about 4.45%. For our simulations the corresponding heat and peak errors were about -1.42 and 0.58%, respectively (Figure 1a). Going further back in time, up to 88% of the simulated time T_{sim} interval, Elden showed about 45.8% heat difference and 50.7% peak difference, while our approximation showed about -28.6% heat difference and 5.21% peak difference (Figure 1b). The temperature distribution at a backward time t_b of $0.88T_{sim}$ showed a good match with the exact value, although we can observe slight phase shifts and minor, but yet extant, change in frequency for both Elden's and MJBBE results. In our solution the difference in phase between the exact solution and the MJBBE solution is more noticeable at $t_b = 0.88T_{sim}$.

4.2. MJBBE Results for the Homogeneous ADE

The next level of complexity for the study of the MJBBE method is to apply it to homogeneous ADE cases. Numerical experiments were conducted for advection-dispersion of a rectangular wave. For every run a forward-time simulation was conducted up to $t = T_{ft} = 2$. The concentration distribution result was then assumed to be the present-day contamination configuration. The length of the domain was $L = 28$. Using the MJBBE method, the concentration configuration at $t = T_{ft} \equiv T_{bi}$ was taken to be $f_2(x)$. Because the method requires one to assume the spatial distribution of the attribute of interest at $t = 0$ to be equal to zero, the spatial distribution at that time will be impossible to be recovered. In our synthetic examples we assumed our terminal time to be $t = T_{bt} = 1$, and there is no concentration distribution for $t < 1$. We want to recover the concentration distribution at $t = T_{target} = 1.1$. In this case, our total time of simulation becomes $T_{sim} = T_{bi} - T_{bt} = 1$. The initial and target concentration distributions can be seen in Figure 2.

The propagation of a rectangular pulse of solute is governed by (18) subject to

$$C(x, 0) = 0 \quad \forall 0 < x < 13.5 \text{ and } 14.5 < x < 28 \quad (38)$$

$$C(x, 0) = C_1 = 1 \quad 13.5 \leq x \leq 14.5. \quad (39)$$

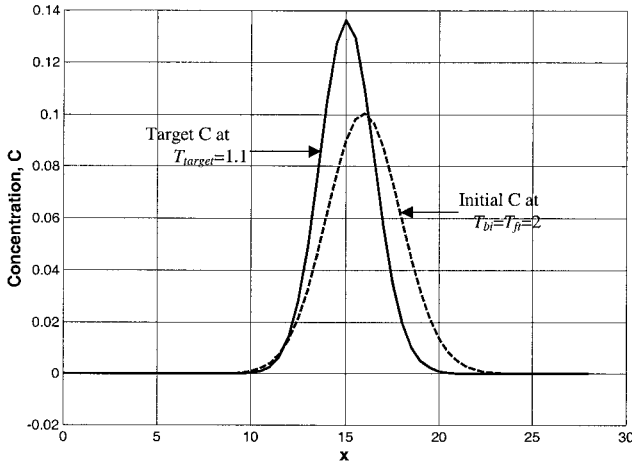


Figure 2. Initial and target concentration distribution for the homogeneous ADE problem.

We solve (18) subject to (38) and (39) using the MJBBE method with $\Delta x = 0.5$ and $\Delta t = 0.02$. In the homogeneous medium case, $D(x)$ and $u(x)$ are set to be constants equal to one for the whole domain. Even though comparisons with analytic solutions are possible, errors of the MJBBE results were compared to the numerical forward solution at different snapshots in time, namely, 20 and 90% back in time (t_b) for consistency purposes. We used $M = \|C(x, 0)\| = 1$, $\delta = 10^{-9}$, and $T_{bi} = 2$, which gives $k \cong 10$. Similar to the backward heat equation example, we used two different measurement errors, which are

(1) mass error, normalized by the exact mass

$$\varepsilon_M = \frac{\text{Mass}^a - \text{Mass}^{\text{num}}}{\text{Mass}^a} \times 100\% \quad (40)$$

(2) concentration peak error, normalized by the exact peak concentration

$$\varepsilon_P = \frac{\max(C^a) - \max(C^{\text{num}})}{\max(C^a)} \times 100\%. \quad (41)$$

In addition to computer time requirement savings, the errors generated by the MJBBE method are slightly lower for a given k value. Mass errors produced by both JBBE and MJBBE are very small for times close to T_{bi} , and grow slightly further back in time. Table 1 shows the errors developed by both MJBBE and JBBE for the homogeneous diffusion case.

In the homogeneous case we studied the movement of the peak concentration for the CFD, UFD, and 3UFD approximations for the velocity term. We performed these analyses because it was not known a priori how the finite difference formulation for the advective term behaved after the ADE was transformed into the backward beam equation. Figure 3 shows the results of the three finite difference approximations and the comparison result obtained via forward simulation. The CFD and 3UFD approximations give the same accuracy in terms of the peak location. At $t_b = 0.2T_{\text{sim}}$ the forward simulation peak is at $x = 16$, and at $t_b = 0.9T_{\text{sim}}$ it is at $x = 15$. The peak position of the plume is exactly the same for the three formulations at $t_b = 0.2T_{\text{sim}}$. As the time progresses backward, that is, at $t_b = 0.9T_{\text{sim}}$, the peak position is the same for both CFD and 3UFD. However, the 3UFD formulation generated larger peak error (Figure 3b). From the same figure we can see that the UFD formulation peak movement

lags behind the forward results. The UFD backward peak is at $x = 15.5$ compared to the forward result for which the peak is at $x = 15$. In addition to the phase lag, the UFD peak error is also larger than for the CFD. Among the three different formulations, UFD is the least accurate in terms of peak position, and the 3UFD method is the least accurate in terms of the peak error. Therefore the central difference method was used to approximate the advective and diffusive parts of the equation.

Figure 3 shows the results of the MJBBE for the homogeneous ADE case. The mass error at $t_b = 0.2T_{\text{sim}}$ is -0.24% , and the peak error is -0.19% (Figure 3a). The recovered concentration distribution at $t_b = 0.9T_{\text{sim}}$ has mass and peak errors of -1.10 and -0.77% , respectively (Figure 3b). *Buzbee and Carasso [1973]* warned that the truncation error term $O(\Delta t^2)$ contained a factor k^4 due to replacing w_{it} by a second-order differencing formula. For the full discrete scheme the truncation error becomes $O[(k^4) \Delta t^2] + O(\Delta x^2)$; that is, the factor k^4 does not affect the error due to discretizing the space variables. Even though we did not perform the same study as Buzbee and Carasso for Δx and Δt , our study confirms their observation. Using smaller values of Δx does not significantly affect the accuracy of the method. Although the accuracy in the peak error is slightly different for $\Delta x = 0.5, 0.25,$ and 0.125 , the mass errors are about the same (Table 2), and the difference in the peak error is negligible. However, reducing

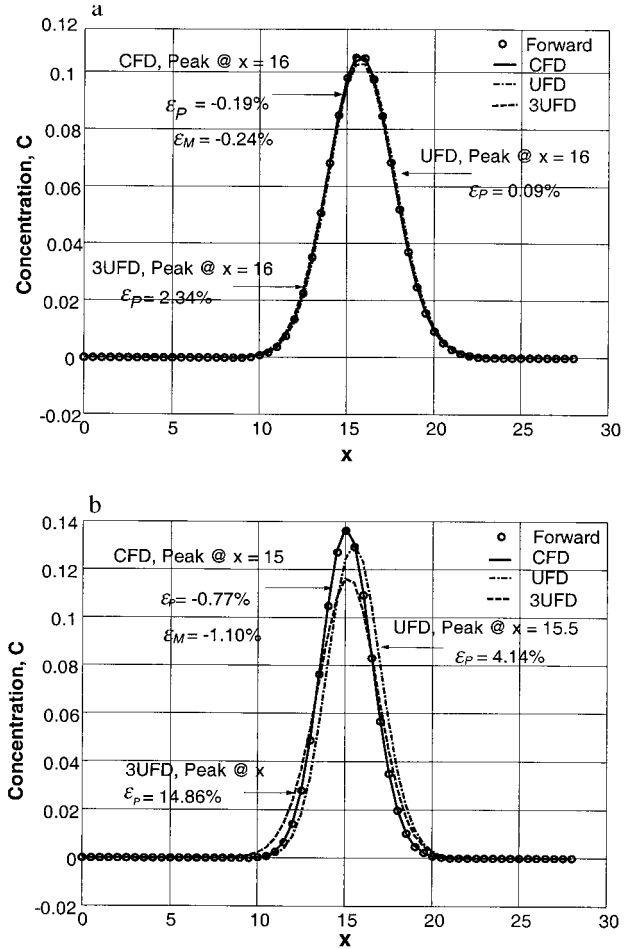


Figure 3. CFD, UFD, and 3UFD formulation study for the MJBBE for homogeneous ADE problem with $t_{\text{tot}} = 0.5$ and $k = 10$ at (a) $t_b = 0.2T_{\text{sim}}$ and (b) $t_b = 0.9T_{\text{sim}}$.

Table 2. Summary of Mass and Peak Errors for Different Δx Values for $\Delta t = 0.02$

Δx	$\varepsilon_M, \%$		$\varepsilon_P, \%$	
	$0.2T_{\text{sim}}$	$0.9T_{\text{sim}}$	$0.2T_{\text{sim}}$	$0.9T_{\text{sim}}$
0.5	-0.24	-1.10	-0.19	-0.77
0.25	-0.24	-1.10	-0.20	-0.75
0.125	-0.24	-1.10	-0.20	-0.81

Δt increases the accuracy of both mass and peak errors. For example, from the results at $t_b = 0.9T_{\text{sim}}$ we observed that the mass error is decreased from -1.10% for $\Delta t = 0.02$ to 0.014% for $\Delta t = 0.01$ (Table 3). However, decreasing it further to $\Delta t = 0.005$ did not improve the MJBBE performance.

4.3. MJBBE Computational Requirements

Using the JBBE for our homogeneous example, the CPU time requirement was 98.01 s. For the original JBBE method, to recover the concentration distribution at $T_{\text{target}} = 1.1$, we have to solve the problem simultaneously from $T_{bi} = 2$ to $T_{bt} = 0$ since using this method we need to use the whole time domain. If $\Delta t = 0.02$ were to be chosen, for a total time of 2, the number of the time discrete points is $N_t = 100$. On the other hand, for the modified JBBE, we do not need to solve the whole time domain simultaneously. For the case where the target time $T_{\text{target}} = 1.1$, we can march the solution to time $t = 1$, and our backward terminal time becomes $T_{bt} = 1$. Our total simulation time becomes $T_{\text{sim}} = 2 - 1 = 1$. The modification to the JBBE was done by choosing a smaller total time and marching the problem backward as described before. This total time will in turn make up for the size of N_t for every marching step. To compare the JBBE requirements with that of the modified method (MJBBE), we performed simulations for different total times and observed the mass error at $t_b = 0.1T_{\text{sim}}$ and $t_b = 0.9T_{\text{sim}}$. The value of t_{tot} was chosen, for a given value of k , to be the smallest time interval where the mass error is close to zero. We first reduced the total time to $t_{\text{tot}} = 0.7$, and the CPU time requirement was reduced to 63.94 s on a dual processor Pentium III 700 MHz computer. The reduction of the CPU time requirement was due to the fact that N_t was reduced from 100 to 35. The mass error at $t_b = 0.1T_{\text{sim}}$ was -0.16% . We reduced the total time further to $t_{\text{tot}} = 0.5$, which in turn reduced the mass error to -0.12% and the CPU time to 30.48 s. Although the CPU time requirement is reduced to 3.53 s for $t_{\text{tot}} = 0.2$, the value of the mass error grows to 17.85% . A summary of the mass errors and CPU time requirements for different time intervals can be found in Table 4. From this exercise we observed that there is an optimum t_{tot} that one must use to obtain a good mass error and shorter CPU

Table 3. Summary of Mass and Peak Errors for Different Δt Values for $\Delta x = 0.5$

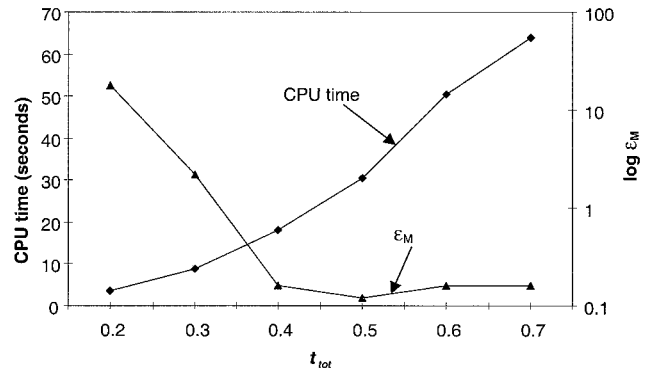
Δt	$\varepsilon_M, \%$		$\varepsilon_P, \%$	
	$0.2T_{\text{sim}}$	$0.9T_{\text{sim}}$	$0.2T_{\text{sim}}$	$0.9T_{\text{sim}}$
0.02	-0.24	-1.10	-0.19	-0.77
0.01	-0.012	0.014	-0.06	0.09
0.005	0.04	0.19	0.06	0.29

Table 4. CPU Time Requirement and Mass and Peak Errors for Different t_{tot} for the MJBBE

t_{tot}	N_t	CPU Time, s	$\varepsilon_M, \%$		$\varepsilon_P, \%$	
			$0.1T_{\text{sim}}$	$0.9T_{\text{sim}}$	$0.1T_{\text{sim}}$	$0.9T_{\text{sim}}$
0.7	35	63.94	-0.16	-1.50	-0.15	-1.30
0.6	30	50.44	-0.16	-1.45	-0.15	-1.24
0.5	25	30.48	-0.12	-1.10	-0.11	-0.77
0.4	20	18.01	0.16	1.41	0.19	2.38
0.3	15	8.83	2.22	18.31	2.39	21.51
0.2	10	3.53	17.85	82.96	18.39	71.00

time requirement (Figure 4). On the basis of these observations one can see that the optimum value occurred when the curves of the mass error and CPU time cross each other at $t_{\text{tot}} = 0.37$. However, we chose $t_{\text{tot}} = 0.5$ for our analysis because it has the least mass error and the CPU time requirement is still reasonably less than that of the JBBE. We then save the results at $t = T_{bi} - \Delta T$, where for our example ΔT is chosen to be 0.1, and the mass error introduced by the method is very small. We then use the results at $t = T_{bi} - \Delta T$ as initial conditions T_i that will be our initial time for the next step and so forth. By incorporating the marching jury method for our particular ADE problem, we were able to reduce the computational requirement from 98.01 to 30.48 s. The computational savings offered by using the MJBBE are evident, especially when we have large problems to solve.

Even though the mass error grows to 17.85% for $t_{\text{tot}} = 0.2$, one can reduce the error by using different k values. For $t_{\text{tot}} = 0.2$, changing the k value from 10 to 24 reduces the mass error from 17.85% to -0.024% and the peak error value from 18.39% to 0.41% at $t_b = 0.2T_{\text{sim}}$ (Figure 5a). One disadvantage of changing the k value to reduce the mass error is that we can no longer use (14) to obtain estimates of k . In addition, the peak error becomes larger compared to the results obtained using a k value as estimated by using (14). In this case, the peak error grows to 2.61% at $t = 0.9T_{\text{sim}}$ (Figure 5b) compared to the peak error of -0.77% obtained by using $k = 10$ and $t_{\text{tot}} = 0.5$ (Figure 3b). Although we can no longer use (14) to estimate the k value, for nonreactive contaminants we can obtain the k value by optimizing the mass error. For conservative contaminants, mass is conserved. Therefore one could compare the numerical value of the mass to the initial input mass without any additional knowledge of the plume history in order to constrain the value of k . This exercise was performed for the

**Figure 4.** Plot of CPU time requirement and mass error for different t_{tot} .

homogeneous case only. Throughout the paper, we use a k value approximated by (14) or a small variation around that value for heterogeneous cases, with the exception of the time release history recovery problem.

4.4. MJBBE Results for the Time Release History Recovery

Once we are able to trace the observed plume $C_T(x)$ backward in time accurately, we can approximate the release history $C_{in}(t_j)$ by calculating the concentration C_i^j at $x_i = x_1$ or any other point in space. We attempted reproducing analyses conducted by *Skaggs and Kabala* [1994], who assumed a “true” contaminant release history as

$$C_{in}(t) = \alpha \exp\left(-\frac{(t-t_\alpha)^2}{2(\sigma_\alpha)^2}\right) + \beta \exp\left(-\frac{(t-t_\beta)^2}{2(\sigma_\beta)^2}\right) + \gamma \exp\left(-\frac{(t-t_\gamma)^2}{2(\sigma_\gamma)^2}\right), \quad (42)$$

where $\alpha = 1$, $\beta = 0.3$, $\gamma = 0.5$, $t_\alpha = 130$, $t_\beta = 150$, $t_\gamma = 190$, $\sigma_\alpha = 5$, $\sigma_\beta = 10$, $\sigma_\gamma = 7$. To make sure that the boundaries did not affect our solutions, instead of having the source located at $x = 0$, we moved it to $x = 50$. The spatial distribution of the present-day contaminant plume is shown in Figure 6. We run (42) to $t = 225$, and this becomes our initial

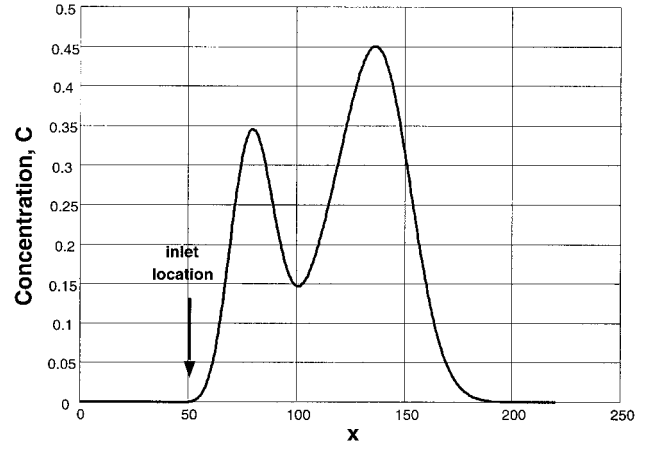


Figure 6. Spatial distribution of Skaggs and Kabala’s plume at $t = T_{bi} = 225$ for the inlet at $x = 50$.

time for the backward problem. Recovering the time history of *Skaggs and Kabala* [1994] was a much more difficult problem to handle with the MJBBE compared to those that have been examined before. The weakness of the MJBBE method is that the mass and peak errors increase over time. For the homogeneous ADE study we were able to obtain good mass and peak errors because the recovery time is relatively short. For the time release history recovery the duration of the release is longer, thereby providing for excessive error growth.

We attempted to recover the release history of the plume shown in Figure 6 from noiseless concentration data. To quantify the errors created by the MJBBE, two different error measurements are calculated for the release history. They are (1) concentration peak error as defined by (41), for each local peak and (2) the error in the location of the peak

$$\epsilon_{XP} = \frac{XP^a - XP^{\text{num}}}{XP^a} \times 100\%, \quad (43)$$

where XP is the location of the peak.

The size of this time history recovery problem is much more significant both in the spatial and temporal domains than the previous homogeneous ADE example. The spatial domain size for this problem is $L = 250$. This is about 9 times larger than the ADE case for which $L = 28$. We chose $\Delta x = 1$ and $\Delta t = 0.2$. If we were to use the JBBE method, we would need to solve the problem simultaneously, and the computational effort would be $O(250^2 \times 1125^2 \times 1)$. Apart from the excessive CPU requirement, this problem would be impossible to solve on most personal computers due to memory limitations. The superiority of the MJBBE method is that one does not need to solve the problem simultaneously over the whole spatial and temporal domains. We can march the problem backward by choosing a smaller t_{tot} to recover the time release history. In this case, we chose $t_{\text{tot}} = 2$ and $\Delta T = \Delta t = 0.2$. By using $t_{\text{tot}} = 2$ the computational effort is reduced to the $O(250^2 \times 10^2 \times 1125)$. In our previous analysis we observed that there is an optimum value of t_{tot} that can be used for a given k value. Using (14), with $T_{bi} = 225$, $M = 1$, and $\delta = 10^{-9}$, the k value is estimated as 0.08. Running the problem one time step back, using $k = 0.08$ produced large mass and peak errors. Therefore we postulated that the total time t_{tot} used in the analysis is too small and we can no longer use the k value as estimated by using (14). The k value was then

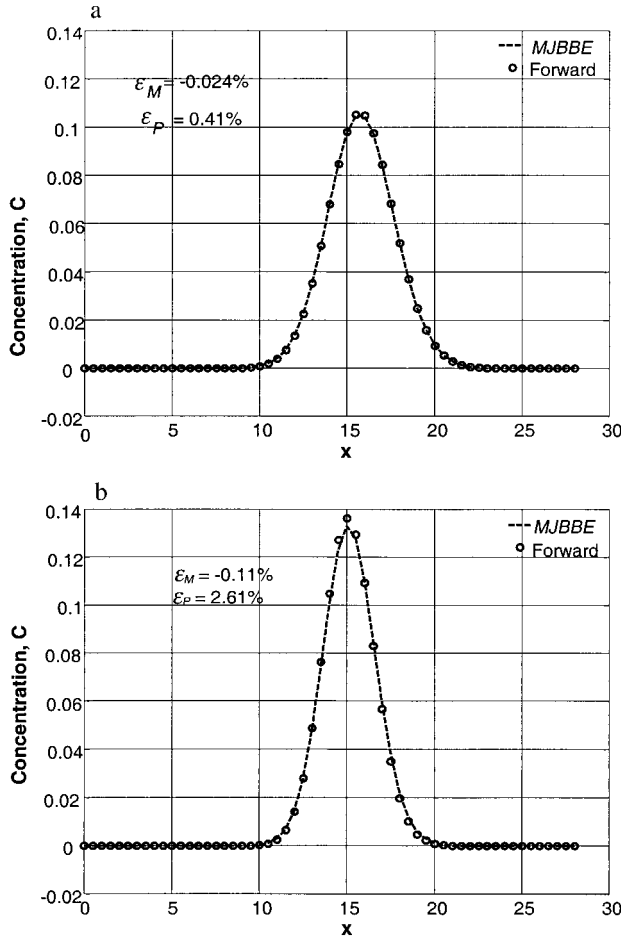


Figure 5. MJBBE method results for homogeneous ADE problem with $t_{\text{tot}} = 0.2$ and $k = 24$ at (a) $t_b = 0.2T_{\text{sim}}$ and (b) $t_b = 0.9T_{\text{sim}}$.

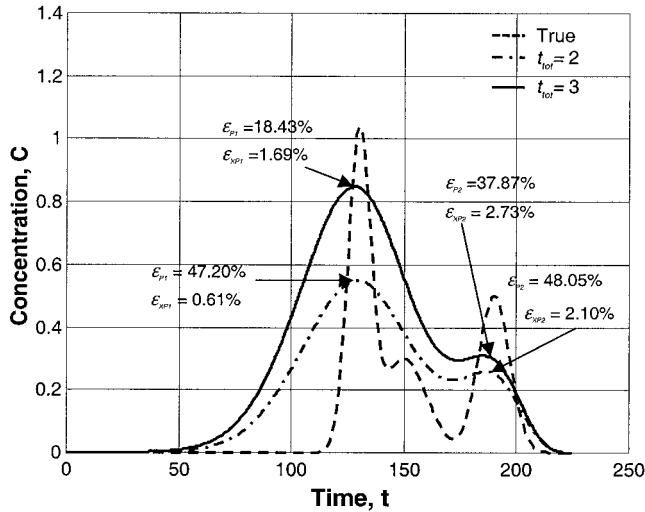


Figure 7. Plume release history recovery using different t_{tot} values.

obtained by running the problem backward for one time step and examining the mass error. The k value that gives mass error close to zero is used to run the problem further backward. Using a single value of k (0.25) and $t_{tot} = 2$, the MJBBE was able to identify the temporal locations of the two larger peaks at $t = 130$ (location 1) and at $t = 190$ (location 2) (Figure 7). The smallest concentration peak at $t = 150$ was not captured by the MJBBE at all. Moreover, the release history recovered by the MJBBE has lower peaks than the true solution. The peak errors are 47.20% for the peak at location 1 and 48.05% for the peak at location 2 (Figure 7). In spite of the large peak errors, the method was able to predict the locations of the peaks fairly accurately, with a peak location error of 0.61% for location 1 and 2.10% for location 2.

Performing a sensitivity study for the total time t_{tot} used in the MJBBE method showed us again that the MJBBE performance depended on t_{tot} . Increasing t_{tot} from 2 to 3 and using the same value of $k = 0.25$, the peak errors are improved, and the values became 18.43 and 37.87% for the peak at locations 1 and 2, respectively (Figure 7). However, the peak location was shifted slightly to the left, especially for location 1, where the error increased from 0.61 to 1.69%. Increasing the total time further to $t_{tot} = 4$ did not improve the MJBBE performance tremendously. The two peak locations remained the same as that of $t_{tot} = 3$. Furthermore, the peak error improvement was insignificant. For peak location 1 the peak error improved from $\epsilon_{P1} = 18.43\%$ for $t_{tot} = 3$ to $\epsilon_{P1} = 17.78\%$ for $t_{tot} = 4$. Similarly, the peak error at location 2 improved slightly from 37.87% for $t_{tot} = 3$ to 37.67% for $t_{tot} = 4$. The results for $t_{tot} = 4$ are not presented here.

Table 5. Dispersion Coefficient Configurations for Heterogeneous ADE

Configuration	D_o	D_i	Inner Zone Width
1	1	8	2
2	1	8	6
3	8	1	6
4	3	1	6

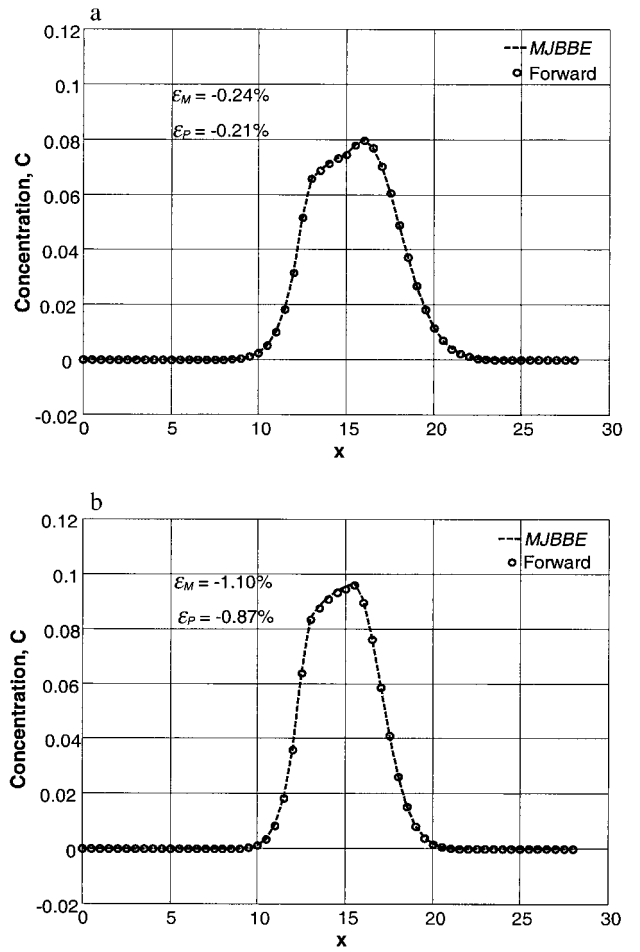


Figure 8. MJBBE method results for configuration 1 at (a) $t_b = 0.2T_{sim}$ and (b) $t_b = 0.9T_{sim}$.

4.5. MJBBE Results for Deterministically Heterogeneous ADE

Four cases involving heterogeneity in the dispersion coefficient D were analyzed. In all the heterogeneous parameter cases the velocity u was set to one. The heterogeneity configurations can be seen in Table 5. Two different zones, each with a distinct value of D , were used. The zones are (1) outer zones for $0 \leq x < 13$ and $15 < x \leq 28$; and (2) inner zone for $13 \leq x \leq 15$ for configuration 1. To study the effect of the inner zone's width, for configurations 2, 3, and 4 we used (1) outer zones for $0 \leq x < 11$ and $17 < x \leq 28$; and (2) inner zone for $11 \leq x \leq 17$. Figures 8 to 11 show the results of the MJBBE for all four configurations. In all cases we first tried to use $k = 10$ as for the homogeneous case based on the bounds M and δ we set earlier. However, we were not able to use the same value of k for all four cases due to the difference in the heterogeneous parameter configurations. The results will be discussed below.

Figure 8 shows a configuration where the inner zone is narrow and has a higher dispersion coefficient than that in the outer zone. In this case, the dispersion coefficient in the inner zone is 8 times higher than that in the outer zones, and the width of the inner zone is 2. We were able to use the same k value as in the homogeneous case. The mass errors created by the MJBBE for both heterogeneous and homogeneous cases at

$t_b = 0.2T_{sim}$ and $t_b = 0.9T_{sim}$ are the same. The values are -0.24% at $t_b = 0.2T_{sim}$ (Figures 3a and 8a) and -1.10% at $t_b = 0.9T_{sim}$ (Figures 3b and 8b). The heterogeneity affected the behavior of the MJBBE by increasing the peak errors slightly; however, the increase is negligible. The peak error at $t_b = 0.2T_{sim}$ is increased from -0.19% for the homogeneous case (Figure 3a) to -0.21% for heterogeneous case 1 (Figure 8a). Similarly, for $t_b = 0.9T_{sim}$ the peak error is increased from -0.77 to -0.87% (Figures 3b and 8b).

A wider inner zone did not significantly affect the performance of the MJBBE. Configuration 2 has an inner zone which is 3 times wider than that of configuration 1. The mass errors at $t_b = 0.2T_{sim}$ and $t_b = 0.9T_{sim}$ are the same as that of configuration 1 (Figure 9). The only noticeable difference is that the numerical peak at $t_b = 0.9T_{sim}$ becomes slightly higher and the peak error becomes worse, with a value of -0.97% (Figure 9b).

When we switched the value of zone 1 and 2, that is $D_o = 8D_i$, we were not able to use the same value of k as before. There are two ways to obtain an estimate for the k value. The first method is to minimize the mass error since, as mentioned earlier, for a nonreactive contaminant the mass is conserved. The second method is to run the problem further forward. In reality, this can be done in the field during a monitoring phase. Once the contaminant plume is discovered, we take measurements of the plume and monitor it for a short period of time.

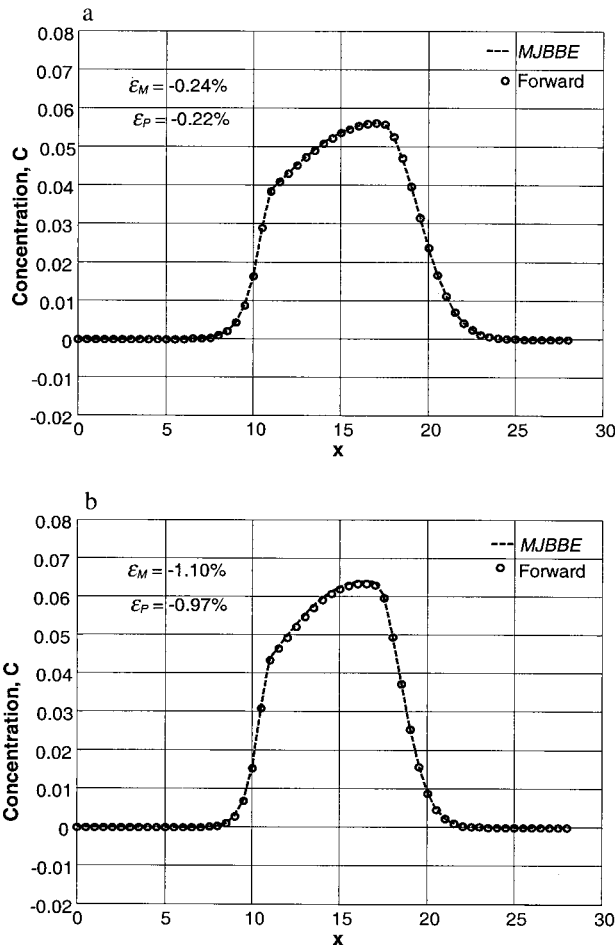


Figure 9. MJBBE method results for configuration 2 at (a) $t_b = 0.2T_{sim}$ and (b) $t_b = 0.9T_{sim}$.

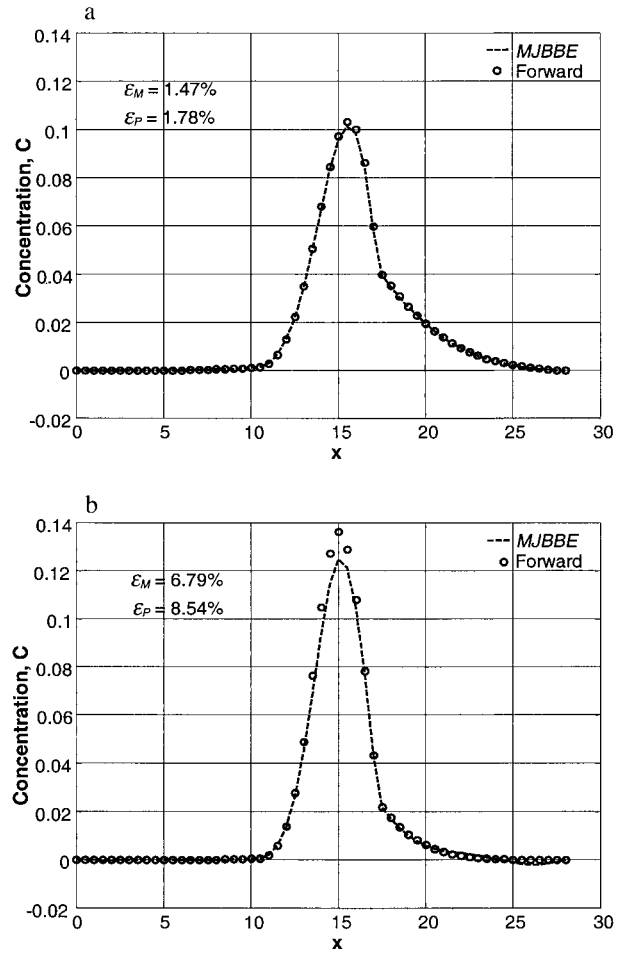


Figure 10. MJBBE method results for configuration 3 at (a) $t_b = 0.2T_{sim}$ and (b) $t_b = 0.9T_{sim}$.

This way we have two or more different snapshots of the contaminant plume. Using these snapshots, we can then obtain the k value and then run the problem further backward.

Using the first method, we obtained $k = 6$ for configuration 3. The values of the mass and peak errors are getting worse further back in time. The mass error grows from 1.47% at $t_b = 0.2T_{sim}$ to 6.79% at $t_b = 0.9T_{sim}$, while the peak error grows from 1.78 to 8.54% (Figure 10). In addition, we start observing a small concentration fluctuation in the vicinity of $x = 25$ to 30 (Figure 10b). We postulate that the large error growth and concentration fluctuation are due to boundary effects. For configuration 3 we have the dispersion coefficient of the outer zone to be 8 times higher than that of the inner zone, rendering the domain too small for this problem. To test our hypothesis, we reduced the outer zone dispersion coefficient (configuration 4). The outer zone has a dispersion coefficient which is only 3 times higher than the inner zone. Figure 11 shows the MJBBE results for configuration 4. The k value for this configuration has changed from 6 to 7. The mass and peak errors are reduced by about 4% , and we no longer have any concentration fluctuations. In addition to reasonably good mass and peak errors, using the MJBBE method, we were able to capture all the essential features of the plume spatial distribution. A summary of the mass and peak errors for different heterogeneity configurations can be found in Table 6.

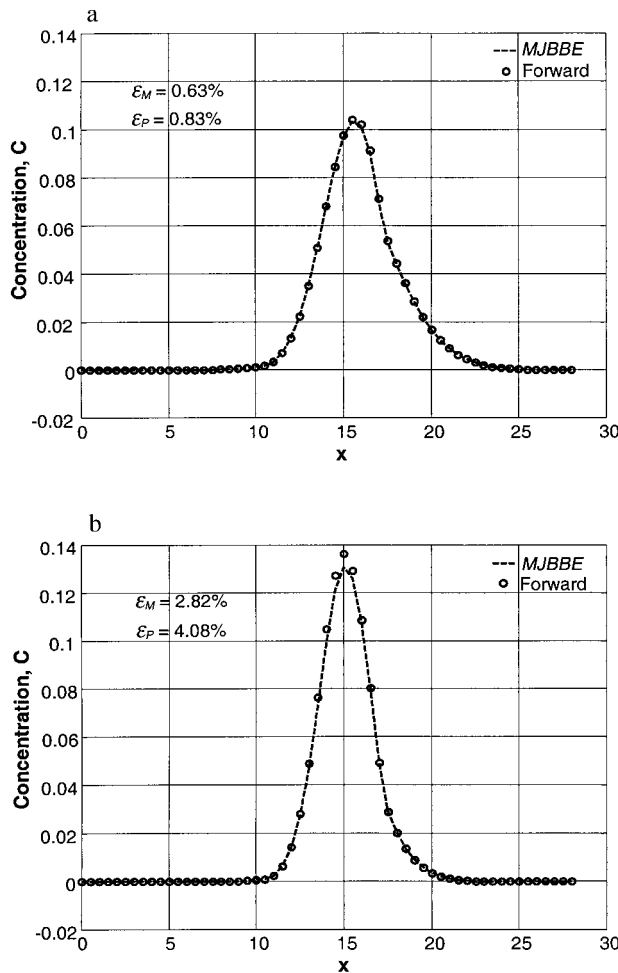


Figure 11. MJBBE method results for configuration 4 at (a) $t_b = 0.2T_{sim}$ and (b) $t_b = 0.9T_{sim}$.

5. Conclusions

The backward beam equation method, as originally proposed by Carasso [1972] and Buzbee and Carasso [1973], was studied and enhanced to solve the 1-D ADE for homogeneous and heterogeneous problems within a contamination source identification context. Several observations from this study are offered below:

1. The MJBBE method introduces a phase shift and a change in frequency into the solution of the backward heat equation example studied.

2. Different finite difference formulations for approximating the advective term affect the accuracy of the solution. The CFD and 3UFD formulations give more accurate results for

Table 6. Summary of Mass and Peak Errors for Heterogeneous ADE Cases

Configuration	k	$\epsilon_M, \%$		$\epsilon_P, \%$	
		$0.2T_{sim}$	$0.9T_{sim}$	$0.2T_{sim}$	$0.9T_{sim}$
1	10	-0.24	-1.10	-0.21	-0.87
2	10	-0.24	-1.10	-0.22	-0.97
3	6	1.47	6.79	1.78	8.54
4	7	0.63	2.82	0.83	4.08

the position of the peak than the UFD formulation. Furthermore, the UFD formulation creates unacceptable phase lags further back in time.

3. Errors in the MJBBE method are consistently lower than that of the JBBE method.

4. The MJBBE method gives very small mass and peak errors for the homogeneous ADE case.

5. The MJBBE method is robust enough to handle heterogeneity. It gives a good accuracy in terms of mass and peak errors. In addition, the method was able to preserve the shape and salient features of the initial data.

6. For some heterogeneous cases the value of k can no longer be estimated a priori using the formula of Buzbee and Carasso [1973]. For conservative tracers, however, the k value can be obtained by minimizing the mass error, without any prior knowledge of the plume history.

7. Owing to the complexity of the shape of the plume and the longer simulation period, reconstruction of the release history of Skaggs and Kabala [1994] was a much more difficult task than for the other cases we examined. The MJBBE was able to recover the larger peaks but was not able to capture the smallest peak at all. However, the method was able to predict the location of the larger peaks to within an error of less than 5%.

8. By using a hybrid between marching and jury methods, we were able to cut down the computational time requirements by about 3 times for the ADE examples presented.

9. Expanding the BBE formulation for the 2-D case we get an auxiliary problem, which is similar to the equation of motion for a plate, hence the name BPE, that can be used to perform plume backtracking in 2-D heterogeneous media.

Acknowledgments. The first author acknowledges the financial support of the Boris A. Bakhmeteff Research Fellowship in Fluid Mechanics and additional computing facility support from the American Petroleum Institute and National Ground Water Association graduate student award. We also want to thank the Associate Editor, Peter Kitanidis, for handling the review process and the three anonymous reviewers for their valuable comments and suggestions on the manuscript.

References

- Alapati, S., and Z. J. Kabala, Recovering the release history of a groundwater contaminant via the non-linear least-squares estimation, *Hydrol. Processes*, 14(6), 1003–1016, 2000.
- Bagtzoglou, A. C., Particle-grid methods with application to reacting flows and reliable solute source identification, Ph.D. dissertation, 246 pp., Univ. of Calif., Irvine, 1990.
- Bagtzoglou, A. C., A. F. B. Tompson, and D. E. Dougherty, Probabilistic simulation for reliable solute source identification in heterogeneous porous media, in *Water Resources Engineering Risk Assessment, NATO ASI Ser., Ser. G*, 29, 189–201, 1991.
- Bagtzoglou, A. C., D. E. Dougherty, and A. F. B. Tompson, Application of particle methods to reliable identification of groundwater pollution sources, *Water Resour. Manage.*, 6, 15–23, 1992.
- Birchwood, R. A., Identifying the location and release characteristics of a groundwater pollution source using spectral analysis, in *Proceedings of the 19th Annual American Geophysical Union Hydrology Days Conference, Colorado State University*, pp. 37–50, Hydrol. Days, Fort Collins, Colo., 1999.
- Buzbee, B. L., and A. Carasso, On the numerical computation of parabolic problems for preceding times, *Math. Comput.*, 27(122), 237–266, 1973.
- Carasso, A., The backward beam equation: Two A-stable schemes for parabolic problems, *SIAM J. Numer. Anal.*, 9(3), 406–434, 1972.
- Carasso, A., The backward beam equation and the numerical compu-

- tation of dissipative equations backwards in time, *MRC Tech. Summary Rep. 1534*, Univ. of Wis., Madison, 1975.
- Elden, L., Time discretization in the backward solution of parabolic equations, II, *Math. Comput.*, 39(159), 69–84, 1982.
- Gorelick, S. M., B. E. Evans, and I. Remson, Identifying sources of groundwater pollution: An optimization approach, *Water Resour. Res.*, 19(3), 779–790, 1983.
- Liu, C., and W. P. Ball, Application of inverse methods to contaminant source identification from aquitard diffusion profiles at Dover AFB, Delaware, *Water Resour. Res.*, 35(7), 1975–1985, 1999.
- Liu, J., and J. L. Wilson, Modeling travel time and source location probabilities in two-dimensional heterogeneous aquifer, in *Proceedings of the 5th WERC Technology Development Conference*, pp. 59–76, Waste Manage. Educ. and Res. Consortium, Las Cruces, N.M., 1995.
- MacDonald, J. R., Solution of an “impossible” diffusion-inversion problem, *Comput. Phys.*, 9(5), 546–553, 1995.
- Mahar, P. S., and B. Datta, Optimal monitoring network and groundwater pollution source identification, *J. Water Resour. Plann. Manage.*, 123, 199–207, 1997.
- Mahar, P. S., and B. Datta, Identification of pollution sources in transient groundwater systems, *Water Resour. Manage.*, 14, 209–227, 2000.
- Mahar, P. S., and B. Datta, Optimal identification of ground-water pollution sources and parameter identification, *J. Water Resour. Plann. Manage.*, 127, 20–29, 2001.
- Morrison, R. D., Application of forensic techniques for age dating and source identification in environmental litigation, *J. Environ. Forensics*, 1(3), 131–153, 2000.
- Neupauer, R. M., and J. L. Wilson, Adjoint method for obtaining backward-in-time location and travel time probabilities of a conservative groundwater contaminant, *Water Resour. Res.*, 35(11), 3389–3398, 1999.
- Neupauer, R. M., B. Borchers, and J. L. Wilson, Comparison of inverse methods for reconstructing the release history of a groundwater contamination source, *Water Resour. Res.*, 36(9), 2469–2475, 2000.
- Skaggs, T. H., and Z. J. Kabala, Recovering the release history of a groundwater contaminant, *Water Resour. Res.*, 30(1), 71–79, 1994.
- Skaggs, T. H., and Z. J. Kabala, Recovering the history of a groundwater contaminant plume: Method of quasi-reversibility, *Water Resour. Res.*, 31(11), 2669–2673, 1995.
- Skaggs, T. H., and Z. J. Kabala, Limitations in recovering the history of a groundwater contaminant plume, *J. Contam. Hydrol.*, 33, 347–359, 1998.
- Snodgrass, M. F., and P. K. Kitanidis, A geostatistical approach to contaminant source identification, *Water Resour. Res.*, 33(4), 537–546, 1997.
- Stout, S. A., A. D. Uhler, T. G. Naymik, and K. J. McCarthy, Environmental forensic unraveling site liability, *Environ. Sci. Technol.*, 32, 260A–264A, 1998.
- Tikhonov, A. N., and V. Y. Arsenin, *Solutions of Ill-Posed Problems*, pp. 7–8, V. H. Winston, Washington, D. C., 1977.
- U.S. Environmental Protection Agency (EPA), Report brochure: National Water Quality Inventory: 1996 report to Congress, background section, Off. of Water, Washington, D. C., 1998a. (Available at <http://www.epa.gov/OW/resources/brochure/broch2.html>)
- U.S. Environmental Protection Agency (EPA), National Water Quality Inventory: 1996 report to Congress, ground water chapters, Off. of Water, Washington, D. C., 1998b. (Available at <http://www.epa.gov/OW/resources/9698/chap6.html>)
- U.S. Environmental Protection Agency (EPA), Safe Drinking Water Act, Section 1429, groundwater report to Congress, *EPA-816-R-99-016*, Off. of Water, Washington, D. C., 1999. (Available at <http://www.epa.gov/safewater/gwr/finalgw.pdf>)
- Wagner, B. J., Simultaneously parameter estimation and contaminant source characterization for coupled groundwater flow and contaminant transport modeling, *J. Hydrol.*, 135, 275–303, 1992.
- Wilson, J. L., and J. Liu, Backward tracking to find the source of pollution, in *Waste Management From Risk to Remediation*, vol. 1, chap. 10, pp. 181–199, ECM, Albuquerque, N. M., 1994.
- Woodbury, A. D., and T. J. Ulrych, Minimum relative entropy inversion: Theory and application to recovering the release history of groundwater contaminant, *Water Resour. Res.*, 32(9), 2671–2681, 1996.
- Woodbury, A., E. Sudicky, T. J. Ulrych, and R. Ludwig, Three-dimensional plume source reconstruction using minimum relative entropy inversion, *J. Contam. Hydrol.*, 32, 131–158, 1998.

J. Atmadja and A. C. Bagtzoglou, Department of Civil Engineering, Columbia University, New York, NY 10027. (abagtzog@civil.columbia.edu)

(Received October 17, 2000; revised February 26, 2001; accepted March 26, 2001.)

